


**Exact solutions for shock waves in dilute gases**F. J. Uribe<sup>✉\*</sup> and R. M. Velasco<sup>†</sup>*Department of Physics, Universidad Autónoma Metropolitana-Iztapalapa 09340, CDMX, México* (Received 5 May 2019; revised manuscript received 15 August 2019; published 28 August 2019)

In 1922 Becker found an exact solution for shock waves in gases using the Navier–Stokes–Fourier constitutive equations for a Prandtl number of value  $3/4$  with constant transport coefficients. His analysis has been extended to study some cases where an implicit solution can be found in an exact way. In this work we consider this problem for the so-called soft-spheres model in which the viscosity and thermal conductivity are proportional to a power of the temperature  $\eta, \kappa \propto T^\sigma$ . In particular, we give implicit exact solutions for the Maxwell model ( $\sigma = 1$ ), hard spheres ( $\sigma = 1/2$ ), and when  $\sigma$  (the viscosity index) is a natural number.

DOI: [10.1103/PhysRevE.100.023118](https://doi.org/10.1103/PhysRevE.100.023118)**I. INTRODUCTION**

The history of the problem we face is long, in fact, the subject of shock waves was founded by Stokes (1819–1903), Earnshaw (1805–1888), Rankine (1820–1872), Hugoniot (1851–1887), and Riemann (1826–1866), among others [1]. Two relevant manuscripts on the subject appeared in 1910, one by Rayleigh [2], who addressed the works of the founders of the subject, including his discussions with Stokes on the subject. The other work by Taylor [3], showed the existence of shock-wave solutions for a fluid with constant viscosity with no thermal conductivity or with constant thermal conductivity but no viscosity. He also provided a perturbative solution for weak shocks in which both transport coefficients were included. A remarkable result was obtained in 1922 when Becker [4,5] showed an implicit shock-wave solution for all Mach numbers, including constant viscosity and thermal conductivity with the restriction that the Prandtl number is fixed and equal to  $3/4$ . In 1944 Thomas [6] used the hard-sphere model to criticize Becker’s conclusion in the sense that for strong shocks the Boltzmann equation cannot be applied. Later on, in 1949 Morduchow and Libby [7] improved the Becker’s work by showing the existence of a complete integral of the energy equation and a maximum in the entropy at the inflection point in the velocity distribution, both results turned out to be relevant. In 2013 Johnson [8] found analytical shock solutions at large and small Prandtl numbers and a year later he [9] obtained closed-form (explicit) shock solutions for some of them and also for some of Becker’s implicit solutions, the same year Myong [10] found implicit solutions for the Maxwell model and the hard sphere model. Exact solutions for a van der Waals gas with  $Pr = 3/4$  have been reported recently [11].

In the works mentioned previously the research was based on the Navier-Stokes equations of hydrodynamics under the continuum hypothesis. However, by 1920 the atomistic model for fluids was already accepted, in addition it was already

known that the Navier-Stokes equations can be obtained from the Boltzmann equation by means of the Chapman-Enskog method to solve it [12]. Due to the fact that in a shock wave abrupt changes occur in a narrow region, there has been always doubt about the validity of the Navier-Stokes constitutive equations in this case. In a classical paper by Gilbarg and Paolucci in 1953 [13] they rejected such statement based on the evidence found by solving the fluid equations. The discussion is not over yet but the emphasis is now on how to improve on the Navier-Stokes hydrodynamics, if feasible, and the search has been rather prolific as we refer briefly below.

By 1950 there were already studies to tackle the shock-wave problem from the Boltzmann equation. One work by Mott-Smith in 1951 [14] relied on an assumption that the distribution function is bimodal and another one by Grad in 1952 [15], that is more in the tradition of hydrodynamics, used the moments method (13 moments) to derive relaxation type equations from the Boltzmann equation. Besides, again in the tradition of hydrodynamics, higher order hydrodynamic equations obtained with the Chapman-Enskog method, Burnett, and super-Burnett equations, were already in consideration by Burnett in 1935 [16] and later on, in 1948, by Wang Chang [17].

Shock-wave phenomena still provides a difficult problem to solve from the continuum point of view. The problem, for dilute gases, can be tackled using the Boltzmann equation and different methods to solve it like the Chapman-Enskog method [12], Grad’s moments method, or probabilistic methods, such as the direct simulation Monte Carlo (DSMC) method [18,19]. Molecular dynamics (MD) [20,21] is not restricted to dilute gases and provides a very flexible tool for studying shock waves in many situations. The computational methods like DSMC and MD provide a direct approach to study shock waves, though the search about the true interaction potential, must be taken into account. A way to go through this problem takes the *ab initio* potential calculations to obtain thermophysical and transport properties, which can be taken to study specific applications as actually has been done recently [22–24].

The situation with the continuum approach has some points that need to be addressed. For example, it is known that

\*paco@xanum.uam.mx

†rmvb@xanum.uam.mx

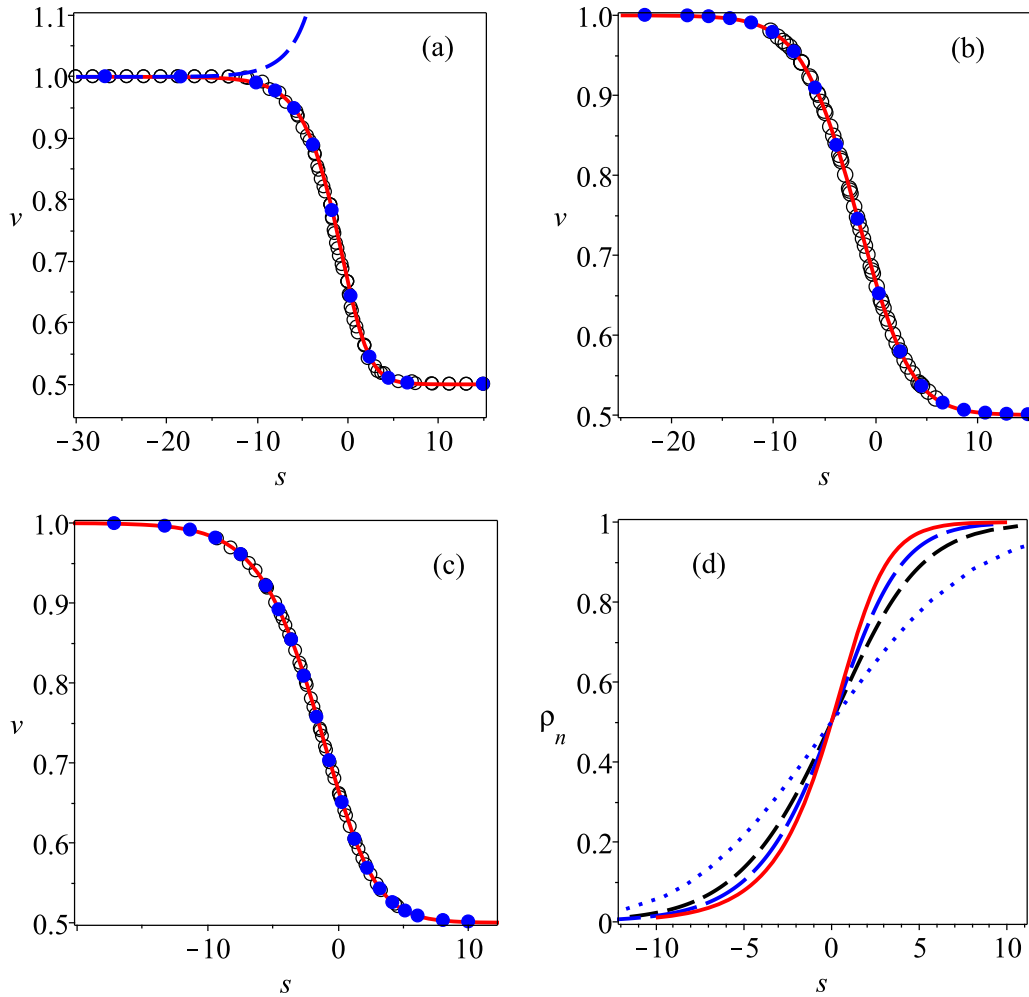


FIG. 1. (a) Explicit and implicit solutions for  $Pr = 3/4$ ,  $\sigma = 0$ , and  $\tau_0 = 1/5$ . Reduced velocity vs the reduced distance,  $v(s)$  vs  $s$ . Solid line: Explicit solution given by Eq. (45); open circles: implicit solution given by Eq. (42); solid circles: numerical solution to Eqs. (15) and (16); dashed line: solution with the plus sign in Eq. (43). (b) Implicit and numerical solutions for  $Pr = 3/4$ ,  $\sigma = 1$ , and  $\tau_0 = 1/5$ . Velocity vs reduced distance,  $v(s)$  vs  $s$ . Open circles: implicit solution given by Eq. (47); solid circles: numerical solution to Eqs. (15) and (16); solid line: numerical solution to Eq. (24) using the initial condition  $v(0) = 2/3$ . (c) Implicit and numerical solutions for  $Pr = 3/4$ ,  $\sigma = 1/2$ , and  $\tau_0 = 1/5$ . Velocity vs reduced distance,  $v(s)$  vs  $s$ . Open circles: implicit solution given by Eq. (47); solid circles: numerical solution to Eqs. (15) and (16) with initial condition  $v(0) = 2/3$  and  $\tau(0) = 14/45$ ; solid line: numerical solution to Eq. (24) using the initial condition  $v(0) = 2/3$ . (d) Normalized density profiles,  $\rho_n$  vs  $s$ , for  $\tau_0 = 1/5$ . Solid line: Becker solution; long dashed line: hard-sphere model; dashed line: Maxwell model; dotted line:  $\sigma = 2$ .

using the Navier-Stokes-Fourier constitutive equations leads to normalized density profiles that are narrow when compared to the experimental values; see Fig. 2. The Chapman-Enskog method provides a methodology to go beyond the previous constitutive equations, they are called Burnett [12,25,26] and super-Burnett equations [27], but the presence of bifurcations for the Burnett equations in the case of shock waves limits their applications [28,29]. Alternatives to the Burnett and super-Burnett equations exist but perhaps they are ad hoc when applied to shock waves [30–34].

In the case of Grad’s method, or moments method in general, the situation is in a sense worse due to the presence of singularities, they imply the non existence of solutions even for small Mach numbers ( $\approx 1.65$ ) like the 13-moment approximation [15] though theories with several thousands of moments have been used [35]. Also, regularizations to the moments method, like R-13, have been considered in

the literature and behave better than the original Grad’s 13-moment equations since they are able to provide shock structure for Mach numbers about 10 [36–38]. For other theoretical approaches using the moments method, see Ref. [39].

Apart from the attempts mentioned, two-fluid, two-velocity, two-temperature, or multiple temperature theories have been proposed with different degree of success. We refer the interested reader to the literature here provided [40–43].

Our objective is to study exact implicit, or explicit when feasible, solutions to the Navier-Stokes-Fourier (NSF) hydrodynamic equations for the soft-sphere model when the Prandtl number is equal to  $3/4$ . Some authors have claimed that such a value for the Prandtl number is not realistic [13], while others say that for air or other systems the Prandtl number is about  $3/4$  [10]. For monatomic gases a more realistic value is  $2/3$  [12,18,19] but in these cases exact solutions are still lacking.

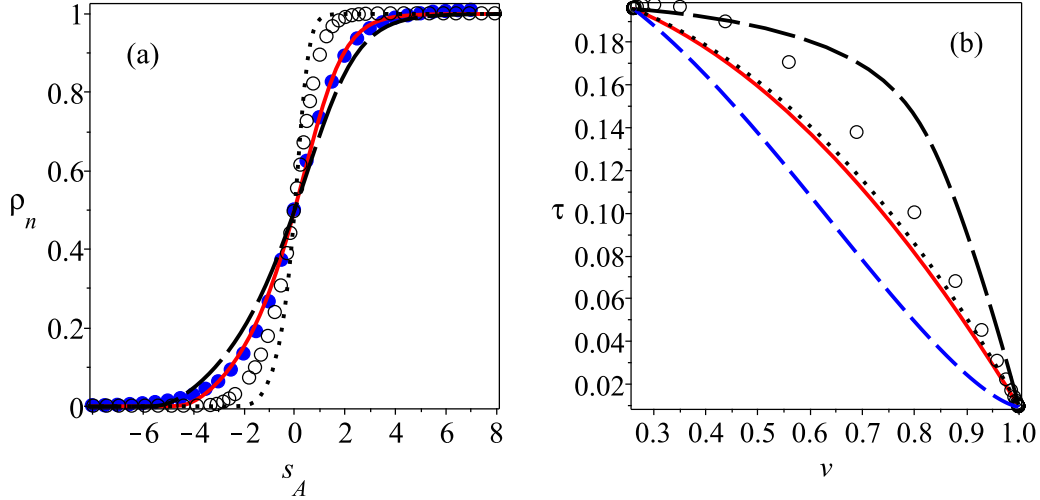


FIG. 2. (a) Normalized density profiles for  $M = 8$ ,  $\rho_n$  vs  $s_A$ , obtained by solving Eq. (24) with initial condition  $v(0) = 134/323$  for different values of  $\sigma$ . Circles: Experiments by Steinhilper [50]; solid line: solution for  $\sigma = 0.92$ ; dotted line: solution for  $\sigma = 1/2$ ; dashed line: solution for  $\sigma = 1$ ; open circles: *ab initio* calculations. (b) Orbits,  $\tau$  vs  $v$ , for  $M = 8$  and different Prandtl numbers. Except for  $\text{Pr} = 3/4$  the orbits were obtained by solving Eqs. (10) with  $\Xi_1 = 1$  and  $\Xi_2 = 15/(8 \text{Pr})$ . Solid line:  $\text{Pr} = 3/4$ , see Eq. (21); dotted line:  $\text{Pr} = 2/3$ ; long dashed line:  $\text{Pr} = 1/10$ ; dashed line:  $\text{Pr} = 2$ ; circles: direct simulation Monte Carlo method for  $\sigma = 0.68$ .

The structure of this work is as follows; after this Introduction, in Sec. II we consider the conservation equations for the shock-wave problem and write the differential equations to be solved without a restriction on the Prandtl number. In Sec. III we provide implicit exact solutions for a Prandtl number of value  $3/4$  with a number of models, whereas in Sec. IV we discuss implicit and explicit exact solutions, and in Sec. V some concluding remarks are given. The Appendix gives a detailed derivation of the shock-wave equations.

## II. THE CONSERVATION EQUATIONS

The description of fluid behavior in the continuum approach starts with the fluxes conservation of mass, momentum, and energy expressions across the shock wave. They will be written in a reference system along the propagation direction which will be taken as the  $x$  axis, in such a case the shock wave is seen as steady. Then they look as follows:

$$\rho u = c_1, \quad (1a)$$

$$\rho u^2 + P_{xx} = c_2, \quad (1b)$$

$$\rho u \left( e + \frac{P_{xx}}{\rho} + \frac{u^2}{2} \right) + q = c_3. \quad (1c)$$

In these equations, the variables  $(\rho, u, e)$  are the mass density, the speed along the propagation direction  $x$ , and the specific energy, respectively. The fluxes  $(P_{xx}, q)$  are the  $xx$  component of pressure tensor and the heat flux in the  $x$  direction. The fluid flow in which the shock wave occurs is characterized by the fact that in one direction, when  $x \rightarrow \infty$ , a thermodynamic equilibrium state where no gradients are present is reached. Also, when  $x \rightarrow -\infty$ , a different thermodynamic equilibrium state is obtained. The constant quantities  $(c_1, c_2, c_3)$  in Eqs. (1) are calculated in the following way. We call  $\rho_0, u_0$ , and  $T_0$  the conditions at the equilibrium state that has lower temperature (the cold part of the shock or up-flow)

and  $\rho_1, u_1$ , and  $T_1$  the conditions at the other equilibrium state (the hot part of the shock or down-flow). It follows that these different conditions are related by Eqs. (1) giving place to the well-known Rankine-Hugoniot jump conditions that take the form

$$\begin{aligned} c_1 &= \rho_0 u_0 = \rho_1 u_1, & c_2 &= \rho_0 u_0^2 + p_0 = \rho_1 u_1^2 + p_1, \\ c_3 &= \rho_0 u_0 \left( e_0 + \frac{p_0}{\rho_0} + \frac{u_0^2}{2} \right) = \rho_1 u_1 \left( e_1 + \frac{p_1}{\rho_1} + \frac{u_1^2}{2} \right), \end{aligned} \quad (2)$$

where  $p$  is the hydrostatic pressure. For an ideal fluid, characterized by the lack of any type of viscosity and thermal conductivity, the two equilibrium points are not joined by a continuous curve but for a viscous and conducting fluid sometimes a differentiable curve joins the equilibrium states (an heteroclinic curve in the mathematical jargon), researchers refer this as saying that the shock wave has structure.

Notice that Eqs. (1) contain more unknowns than equations and must be supplemented by the state and the caloric equations in terms of local variables. In addition, the constitutive equations for the “fluxes,” which can be given in terms of gradients or relaxation type equations like in Grad’s moments method.

Here, the constitutive equations will be the Navier-Stokes-Fourier equations written for the one-dimensional case,

$$P_{xx} = p - \frac{4\eta}{3} \frac{\partial u}{\partial x} - \zeta \frac{\partial u}{\partial x}, \quad (3a)$$

$$q = -\kappa \frac{\partial T}{\partial x}, \quad (3b)$$

where  $\eta$  is the shear viscosity,  $\zeta$  is the bulk viscosity, and  $\kappa$  is the thermal conductivity. The shear viscosity and thermal conductivity will be modeled by the soft-sphere model, for which

$$\eta \propto T^\sigma \quad \text{and} \quad \kappa \propto T^\sigma, \quad (4)$$

where we will call  $\sigma$  the temperature-viscosity index or simply the viscosity index. However, it is usually assumed that for dilute monatomic gases the bulk viscosity is zero, a hypothesis which we will also adopt in this work. It must be said that to our knowledge there is at least a work in which the author has introduced a bulk viscosity for this case [44].

To go further, we found convenient to work with a reduced variables velocity, density, temperature and distance defined as follows:

$$v \equiv \frac{u}{u_0}, \quad \rho^* \equiv \frac{\rho}{\rho_0}, \quad \tau \equiv \frac{k_B T}{m u_0^2}, \quad s \equiv \frac{x}{\lambda}, \quad (5)$$

where  $k_B$  is the Boltzmann constant,  $m$  is the molecular mass, and  $\lambda$  is a characteristic length, which is left unspecified for the moment since different values for it are used in the literature. Then, for an ideal fluid and according to the NSF constitutive equations with no bulk viscosity, the reduced forms of  $P_{xx}$  and  $q$  are written as

$$P_{xx}^* \equiv \frac{P_{xx}}{\rho_0 u_0^2} = \frac{\frac{\rho k_B T}{m} - \frac{4}{3} \eta \frac{du}{dx}}{\rho_0 u_0^2} = \frac{\tau}{v} - \left( \frac{4 \eta_0}{3 \lambda \rho_0 u_0} \right) \eta^* \frac{dv}{ds},$$

$$q^* \equiv \frac{q}{\rho_0 u_0^3} = - \left( \frac{\kappa_0 m}{k_B \lambda \rho_0 u_0} \right) \kappa^* \frac{d\tau}{ds}, \quad (6)$$

where  $\eta^* = \eta/\eta_0$  with  $\eta_0$  a reference viscosity and  $\kappa^* = \kappa/\kappa_0$  with  $\kappa_0$  a reference thermal conductivity. Substitution of the previous reduced  $xx$  component of the pressure tensor and the reduced form of the heat flux into the integrated forms of momentum and energy conservation, see Eqs. (1), leads to

$$\frac{\tau}{v} - \left( \frac{4 \eta_0}{3 \lambda \rho_0 u_0} \right) \eta^* \frac{dv}{ds} = (1 + \tau_0) - v, \quad (7a)$$

$$\left[ \frac{5}{2} \tau - \left( \frac{4 \eta_0}{3 \lambda \rho_0 u_0} \right) v \eta^* \frac{dv}{ds} + \frac{v^2}{2} \right] - \left( \frac{\kappa_0 m}{k_B \lambda \rho_0 u_0} \right) \kappa^* \frac{d\tau}{ds} = \frac{5}{2} \tau_0 + \frac{1}{2}. \quad (7b)$$

Notice that we have taken the ideal gas law  $p = \rho k_B T/m$  and for specific internal energy the value  $e = 3 k_B T/2m$  that are true for a monatomic gas.

### The dynamical system

Now we discuss the previous implicit differential equations obtained for an ideal monatomic gas using the NSF constitutive equations. In matrix form the implicit dynamical system given by Eqs. (7) takes the form,

$$\begin{pmatrix} \Xi_1 \eta^* & 0 \\ \Xi_1 v \eta^* & \Xi_2 \kappa^* \end{pmatrix} \begin{pmatrix} \frac{dv}{ds} \\ \frac{d\tau}{ds} \end{pmatrix} = \begin{pmatrix} \frac{\tau + v^2 - (1 + \tau_0)v}{v} \\ \frac{5(\tau - \tau_0) + v^2 - 1}{2} \end{pmatrix}, \quad (8)$$

where

$$\Xi_1 = \left( \frac{4 \eta_0}{3 \lambda \rho_0 u_0} \right) \quad \text{and} \quad \Xi_2 = \left( \frac{\kappa_0 m}{k_B \lambda \rho_0 u_0} \right). \quad (9)$$

Noting that the 2 by 2 matrix that appears in the left hand of Eq. (8) has an inverse, the system can be solved to obtain the following result:

$$\frac{dv}{ds} = \frac{\tau + v^2 - (1 + \tau_0)v}{\Xi_1 v \eta^*}, \quad (10a)$$

$$\frac{d\tau}{ds} = \frac{-v^2 + 2v(\tau_0 + 1) - 5\tau_0 + 3\tau - 1}{2\Xi_2 \kappa^*}. \quad (10b)$$

Numerical methods are usually necessary to solve Eqs. (10) once the values of  $\rho_0$ ,  $u_0$ ,  $\eta_0$ ,  $\kappa_0$ ,  $m$ , and  $\lambda$  are given. However, there are some results that readily follow without numerically solving the equations. First, the critical points of the dynamical system Eqs. (10) are obtained immediately when both derivatives are zero, their coordinates follow in a direct way,

$$P_{\text{up}} \equiv (v_0, \tau_0) = (1, \tau_0) \quad \text{and} \quad P_{\text{down}} \equiv (v_1, \tau_1) = \left( \frac{1 + 5\tau_0}{4}, \frac{-5\tau_0^2 + 14\tau_0 + 3}{16} \right), \quad (11)$$

that can be shown to be the Rankine-Hugoniot jump conditions, see Eqs. (2), expressed in terms of reduced variables. Second, the trajectories in the phase space  $(v, \tau)$  can be obtained, in particular the heteroclinic one, which gives  $\tau$  as a function of  $v$  between the two critical points, called as the ‘‘orbit’’ is obtained as

$$\frac{d\tau}{dv} = \frac{v[-v^2 + 2v(\tau_0 + 1) - 5\tau_0 + 3\tau - 1]}{\tau + v^2 - (1 + \tau_0)v} \frac{4}{15} \text{Pr} \frac{\eta^*}{\kappa^*}, \quad (12)$$

where  $\frac{\Xi_1}{2\Xi_2} = \frac{2}{3} \frac{\eta_0 k_B}{\kappa_0 m} = \frac{4}{15} \text{Pr}$  and the Prandtl number at up-flow is given as  $\text{Pr} = \frac{5}{2} \frac{k_B \eta_0}{m \kappa_0}$ . A first conclusion is that the orbit is independent of  $\lambda$ . Second, if  $\eta = \eta_0 f(\tau/\tau_0)$  and  $\kappa = \kappa_0 f(\tau/\tau_0)$  with  $f(1) = 1$ , then it follows that  $\eta^* = \kappa^*$  as happens for the soft-sphere model. As a consequence, the orbit equation as written in Eq. (12) only depends on the Mach and Prandtl numbers. The form of the orbits for different Prandtl numbers is provided in Fig. 2(b) for  $M = 8$  and they can have very different behavior. In principle, if experimental information for the orbits were available, it could discriminate what would be the Prandtl number, for a given Mach number, that is consistent with the experiments. In the absence of such information the DSMC method provides a clue, from Fig. 2(b) we infer that neither  $\text{Pr} = 3/4$  nor  $\text{Pr} = 2/3$  are consistent with the DSMC information and also that the orbits for such Prandtl numbers are not too different. We emphasize that in this case the orbit does not depend on the viscosity index. Actually, these results can be generalized when the transport coefficients also depend on the density as the reader can show. Such set of characteristics provides a testable prediction that can be used to verify the numerical methods.

A solution to the shock wave is a boundary value problem consisting in finding a solution to Eqs. (10) and (12) that joins the critical points given by Eqs. (11) (this is called an heteroclinic trajectory or orbit in the mathematical jargon). To obtain an approximation to it the Gilbarg–Paolucci method is usually used, it consists in appropriately perturbing slightly down-flow to reach up-flow, detailed explanations are available in the literature [13]. Incidentally, the existence proof

of shock-wave solutions for the NSF hydrodynamic equations was given by Gilberg in 1951 [45].

In our case we use as a perturbation  $(v_1 + 10^{-10}, \tau_1)$  and perform the numerical integration. In the following section we provide the results of numeric computations and compare with experimental data. In addition to the election of  $\lambda$  to reduce the distance the election of the origin to measure  $x$  can be different, this also can be taken into account when comparing with the experimental information.

### III. EXACT SOLUTIONS

To describe the shock-wave structure as given in Eqs. (10) we usually require numerical methods due to their nonlinearity and the presence of the boundary conditions we mentioned above. In the search for solutions, there are some papers which have done a lot of effort to find exact solutions even for specific cases as was mentioned in the Introduction. In particular, when one of the constant transport coefficients is zero, the viscosity or the thermal conductivity, exact solutions are available as was shown by Taylor [3,46]. Another exact solution is the one by Becker [4,7] for constant transport coefficients with a Prandtl of value  $\text{Pr} = 3/4$ . Johnson [8,9] found explicit solutions for constant transport coefficients in the limits  $\text{Pr} \rightarrow 0$  and  $\text{Pr} \rightarrow \infty$ , Myong [10] gave a solution to the Maxwell and hard-sphere model and, Hamad [47] found closed-form solutions for the soft-sphere model when there is not thermal conductivity.

Now let us take the characteristic length to reduce the distance and the Prandtl number as

$$\lambda = \frac{4}{3} \frac{\eta_0}{\rho_0 u_0}, \quad \text{Pr} = \frac{5}{2} \frac{k_B \eta_0}{m \kappa_0}, \quad (13)$$

in this case

$$\Xi_1 = 1, \quad \Xi_2 = \frac{15}{8\text{Pr}}, \quad (14)$$

and we consider that the temperature dependence in the viscosity and the thermal conductivity is the same, so that  $\eta^* = \kappa^*$  then Eqs. (10) can be rewritten as follows:

$$\eta^* \frac{dv^2}{ds} = 2[\tau + v^2 - (1 + \tau_0)v], \quad (15)$$

$$5\eta^* \frac{d\tau}{ds} = \frac{4}{3}\text{Pr}[2v(1 + \tau_0) - (1 + 5\tau_0) - v^2 + 3\tau], \quad (16)$$

adding the previous two equations we obtain

$$\eta^* \frac{d}{ds}(v^2 + 5\tau) = 2v(1 + \tau_0) \left( \frac{4}{3}\text{Pr} - 1 \right) + v^2 \left( 2 - \frac{4}{3}\text{Pr} \right) + \tau(2 + 4\text{Pr}) - \frac{4}{3}\text{Pr}(1 + 5\tau_0), \quad (17)$$

then it is clear that the special value  $\text{Pr} = 3/4$  reduces Eq. (17) to a complete integral that satisfies the following differential equation,

$$\frac{d}{ds} \left( \frac{v^2}{2} + \frac{5\tau}{2} \right) - \frac{1}{\eta^*} \left( \frac{v^2}{2} + \frac{5\tau}{2} \right) = -\frac{1}{\eta^*} \left( \frac{1}{2} + \frac{5\tau_0}{2} \right). \quad (18)$$

It was noticed by Libby and Morduchow [7] that the integral of Eq. (18) comes mainly from the energy equation, in fact

it gives the sum of the kinetic energy per unit mass and the specific enthalpy in the system as a function of  $s$ ,

$$g(s) \equiv \frac{1}{2} v(s)^2 + \frac{5}{2} \tau(s) = C_1 \exp[\phi_\eta(s)] + \frac{5}{2} \tau_0 + \frac{1}{2}, \quad (19)$$

where we will keep the  $s$  dependence for clarity in what follows and  $\phi_\eta(s)$  is a primitive of  $1/\eta^*$ :

$$\frac{d\phi_\eta(s)}{ds} = \frac{1}{\eta^*(s)}. \quad (20)$$

There is no need to determine  $\phi_\eta(s)$  since as Morduchow and Libby noticed; if one is interested in a shock wave one must choose  $C_1 = 0$ , otherwise the solution will not go to a constant as  $s \rightarrow \pm\infty$ , this can be easily verified for  $\sigma = 0$  because in this case  $\phi_\eta(s) = s + C_2$ . Therefore, for a shock wave we have that

$$\tau(s) = \frac{1}{5} + \tau_0 - \frac{v(s)^2}{5}. \quad (21)$$

It is worth noticing that in the phase space  $(v, \tau)$ , Eq. (21) represents the orbit in such a plane. It shows that the orbit is a parabola for any value of the Mach number  $M$  and it is not necessary to solve any differential equations to calculate it. This exact result is clearly consistent with the fact that if  $\eta^* = \kappa^*$ , the orbit should be independent of the viscosity as mentioned previously.

Going further we substitute Eq. (21) into the equation for conservation of momentum, the first one of Eqs. (10) and it leads to

$$\begin{aligned} \frac{dv(s)}{ds} &= \frac{4v(s)^2 - 5\tau_0 v(s) - 5v(s) + 5\tau_0 + 1}{5\eta^*(s)v(s)} \\ &\Rightarrow \frac{5\frac{dv(s)}{ds}\eta^*(s)v(s)}{4[v(s)-1][v(s)-v_1]} = 1, \end{aligned} \quad (22)$$

recall that  $v_1 = (5\tau_0 + 1)/4$ . For the soft-sphere case,

$$\begin{aligned} \eta^*(s) &= (\tau/\tau_0)^\sigma = \frac{[\frac{1}{5} + \tau_0 - \frac{v(s)^2}{5}]^\sigma}{\tau_0^\sigma} \\ &= \frac{1}{5^\sigma \tau_0^\sigma} [1 + 5\tau_0 - v(s)^2]^\sigma = \frac{1}{5^\sigma \tau_0^\sigma} [4v_1 - v(s)^2]^\sigma. \end{aligned} \quad (23)$$

Then, for the soft-sphere model Eq. (22) takes the form

$$\frac{\frac{dv(s)}{ds} [4v_1 - v(s)^2]^\sigma v(s)}{[v(s)-1][v(s)-v_1]} = \frac{4}{5} 5^\sigma \tau_0^\sigma. \quad (24)$$

To obtain implicit solutions in terms of elementary functions we find a primitive of the left hand side of the previous Equation. In other words, if  $F_\sigma(s)$  satisfies

$$\frac{dF_\sigma(s)}{ds} = \frac{dv}{ds} \frac{[4v_1 - v(s)^2]^\sigma v(s)}{[v(s)-1][v(s)-v_1]}, \quad (25)$$

then

$$F_\sigma(s) = \frac{4}{5} 5^\sigma \tau_0^\sigma (s - s_\sigma) \quad (26)$$

is a solution to the differential Eq. (24) where  $s_\sigma$  is an integration constant that in some cases can be taken equal to zero.

To exhibit implicit solutions for the soft-sphere model when  $\sigma \in \mathbb{N} \cup \{0\}$  first we prove the following statement:

*Proposition 1.* Let

$$J_n[v_1, v(s)] \equiv \frac{v_1^{2n+1}}{v_1 - 1} \ln[v(s) - v_1] - \frac{\ln[1 - v(s)]}{v_1 - 1}$$

and  $P_n(v_1, v) = \sum_{k=1}^{2n} c_{n,k}(v_1) \frac{v(s)^k}{k}$ , (27)

where

$$c_{n,k}(v_1) = \frac{v_1^{2n+1-k} - 1}{v_1 - 1} \quad \text{with } n \in \mathbb{N}. \quad (28)$$

Then, if

$$G_n(v_1, v) \equiv P_n(v_1, v) + J_n(v_1, v), \quad (29)$$

the derivative of  $G_n$  with respect to  $s$  satisfies,

$$\frac{dG_n}{ds} = \frac{\frac{dv}{ds} v^{2n+1}}{(v - 1)(v - v_1)}. \quad (30)$$

*Proof.*

$$\frac{dG_n}{ds} = \frac{dP_n}{ds} + \frac{dJ_n}{ds} = \frac{dv}{v_1 - 1} \left\{ \left[ \sum_{k=1}^{2n} (v_1^{2n+1-k} - 1) v(s)^{k-1} \right] + \frac{v_1^{2n+1}}{v(s) - v_1} + \frac{1}{1 - v(s)} \right\}. \quad (31)$$

But

$$\sum_{k=1}^{2n} v_1^{2n+1-k} v(s)^{k-1} = v_1^{2n} \sum_{k=1}^{2n} \left[ \frac{v(s)}{v_1} \right]^{k-1} = v_1^{2n} \left\{ \frac{v_1^2}{v(s)[v(s) - v_1]} \left[ \frac{v(s)}{v_1} \right]^{2n+1} - \frac{v_1}{v(s) - v_1} \right\} = \frac{v_1 v(s)^{2n}}{v(s) - v_1} - \frac{v_1^{2n+1}}{v(s) - v_1}, \quad (32)$$

and

$$\sum_{k=1}^{2n} v(s)^{k-1} = \frac{v(s)^{2n}}{v(s) - 1} - \frac{1}{v(s) - 1}. \quad (33)$$

Substitution of Eqs. (32) and (33) into Eq. (31) gives

$$\begin{aligned} \frac{dG_n}{ds} &= \frac{dv}{v_1 - 1} \left[ \frac{v_1 v(s)^{2n}}{v(s) - v_1} - \frac{v_1^{2n+1}}{v(s) - v_1} - \frac{v(s)^{2n}}{v(s) - 1} + \frac{1}{v(s) - 1} + \frac{v_1^{2n+1}}{v(s) - v_1} + \frac{1}{1 - v(s)} \right] \\ &= \frac{dv}{v_1 - 1} v(s)^{2n} \left[ \frac{v_1}{v(s) - v_1} - \frac{1}{v(s) - 1} \right] = \frac{dv}{v_1 - 1} v(s)^{2n} \frac{v(s)(v_1 - 1)}{[v(s) - 1][v(s) - v_1]} = \frac{\frac{dv}{ds} v^{2n+1}}{(v - 1)(v - v_1)}, \end{aligned} \quad (34)$$

which completes the proof. ■

We are now in position to find solutions to the soft-sphere model when  $\sigma \in \mathbb{N}$ . If  $\sigma \equiv n \in \mathbb{N}$ , then we use the binomial theorem in Eq. (24) to obtain that

$$\frac{dv}{ds} \frac{[4v_1 - v(s)^2]^n v(s)}{[v(s) - 1][v(s) - v_1]} = \sum_{l=0}^n \binom{n}{l} (4v_1)^{n-l} (-1)^l \frac{\frac{dv}{ds} v(s)^{2l} v(s)}{[v(s) - 1][v(s) - v_1]} = \sum_{l=0}^n (-1)^l \binom{n}{l} (4v_1)^{n-l} \frac{dG_l}{ds} = \frac{4}{5} 5^\sigma \tau_0^\sigma. \quad (35)$$

Integration of the last equality with respect to  $s$  leads to the implicit solution

$$F_n(s) = (4v_1)^n G_0(v_1, v) + \sum_{l=1}^n (-1)^l \binom{n}{l} (4v_1)^{n-l} G_l(v_1, v) = \frac{4}{5} 5^n \tau_0^n (s - s_\sigma), \quad (36)$$

where  $s_\sigma$  is an integration constant and  $G_0$  is given by Eq. (38). Then, using Eqs. (27), (28), and (29), we have that

$$\begin{aligned} \frac{4}{5} 5^\sigma \tau_0^\sigma (s - s_\sigma) &= \sum_{l=1}^n (-1)^l \binom{n}{l} (4v_1)^{n-l} \left\{ \frac{v_1^{2l+1}}{v_1 - 1} \ln[v(s) - v_1] - \frac{\ln[1 - v(s)]}{v_1 - 1} + \sum_{k=1}^{2l} \frac{v_1^{2l+1-k} - 1}{v_1 - 1} \frac{v(s)^k}{k} \right\} \\ &\quad + \frac{(4v_1)^n}{v_1 - 1} [v_1 \ln[v(s) - v_1] - \ln[1 - v(s)]] \end{aligned} \quad (37)$$

is an implicit solution of Eq. (24) for  $\sigma = n \in \mathbb{N}$ . Equation (37) provides implicit solutions for any  $\sigma = n \in \mathbb{N}$ , of course for large values of  $n$  the expression has a large number of terms and can be difficult to handle. The number of implicit solutions found is a countably infinite set.

**IV. EXPLICIT AND IMPLICIT SOLUTIONS**

We now illustrate some solutions obtained from Eq. (37) when we take some particular values for the viscosity index.

(1) Let us begin with the case  $\sigma = 0$ , which corresponds to Becker’s solution for constant transport coefficients. In this case, the solution can be obtained directly by the integration of Eq. (24) or by means of the application of Eq. (37) with the convention that  $P_0(v_1, v) = 0$ . Then

$$G_0(v_1, v) = F_0(s) = \frac{v_1 \ln[v(s) - v_1] - \ln[1 - v(s)]}{(v_1 - 1)}. \quad (38)$$

Moreover,

$$F_0(s) = \frac{4}{5}(s - s_0), \quad (39)$$

then, the implicit solution is given as

$$\frac{v_1 \ln[v(s) - v_1] - \ln[1 - v(s)]}{(v_1 - 1)} = \frac{4}{5}(s - s_0), \quad (40)$$

where  $s_0$  can be chosen to satisfy the condition that the normalized density, defined below, has a specific value at  $s = 0$ ,

$$\rho_n(s) = \frac{[1/v(s) - 1]}{[1/v_1 - 1]}, \quad \rho_n(s = 0) = 1/2, \quad (41)$$

as it is usual.

When we take the value  $\tau_0 = 1/5$  so that  $v_1 = 1/2$ , and  $s_0$  with its corresponding value, Eq. (40) drives to the implicit Becker’s solution which can be solved for  $v(s)$  to obtain its explicit expression [4,5,14],

$$\frac{1}{2} \frac{\ln(v(s) - 1/2)}{1/2 - 1} - \frac{\ln[1 - v(s)]}{1/2 - 1} = \frac{4}{5}(s - s_0). \quad (42)$$

From which we obtain

$$v(s) = 1 + \frac{1}{2} e^{\frac{4(s-s_0)}{5}} \pm \frac{1}{2} \sqrt{\left[ e^{\frac{4(s-s_0)}{5}} \right]^2 + 2 e^{\frac{4(s-s_0)}{5}}}. \quad (43)$$

The root corresponding to the minus sign should be chosen since it is the one that provides the asymptotic conditions for a shock wave,

$$\lim_{s \rightarrow \infty} v(s) = \frac{1}{2} \quad \text{and} \quad \lim_{s \rightarrow -\infty} v(s) = 1. \quad (44)$$

Therefore, the explicit shock-wave solution for the example considered is

$$v(s) = 1 + \frac{1}{2} e^{\frac{4(s-s_0)}{5}} - \frac{1}{2} \sqrt{\left[ e^{\frac{4(s-s_0)}{5}} \right]^2 + 2 e^{\frac{4(s-s_0)}{5}}}, \quad (45)$$

where the constant  $s_0 = -(5/4) \ln \frac{2}{3}$  is determined according to Eq. (41).

Johnson [9] showed that for some cases Becker’s implicit solution gives rise to a polynomial in  $v(s)$  and analyzed the conditions under which Becker’s implicit solution can be inverted to provide explicit solutions. Since Abel (1802–1829) and Galois (1811–1832) proved the impossibility of obtaining the roots of any polynomial of degree five in terms of radicals (called the insolubility of the quintic) [48], presumably he looked for conditions under which Becker’s implicit solution gives rise to a polynomial of degree less than five that can be solved in terms of radicals. However, it is in principle possible to find other exact solutions when the degree of the polynomial is greater than four. Johnson’s results were expressed in terms of the compression ratio  $R \equiv \rho_1/\rho_0 = 1/v_1 = 4/(1 + 5\tau_0)$ , a quantity that some researchers prefer to use when dealing with shock waves. In terms of  $\tau_0$ , Johnson’s results are the following: For  $\tau_0 = 1/15 (R = 3)$  or  $1/3 (R = 3/2)$ , Becker’s solution gives rise to a polynomial of third degree, for  $\tau_0 = 0 (R = 4)$  or  $2/5 (R = 4/3)$ , the polynomial is of fourth order as the reader can verify. The particular case considered here and below,  $\tau_0 = 1/5$ , corresponds to a two fold compression ( $R = 2$ ).

(2) The Maxwell model is obtained with  $\sigma = 1$ , the implicit solution follows from Eq. (37) when  $\sigma = n = 1$  and, it can also be obtained by means of the direct integration in Eq. (24) as it was done by Myong in 2014 [10]. We obtain that

$$-\frac{v(s)^2}{2} - (1 + v_1)v(s) + \frac{(-v_1^3 + 4v_1^2)}{v_1 - 1} \ln[v(s) - v_1] + \frac{(-4v_1 + 1)}{v_1 - 1} \ln[1 - v(s)] = 4\tau_0(s - s_1), \quad (46)$$

as the reader can verify. It is a particular case of an implicit solution found by us for  $\sigma \in \mathbb{N}$  as discussed above; see Eq. (37). In this case, as well as in other situations, the process of obtaining the explicit solution from the implicit one can be more difficult than the case illustrated for constant transport coefficients for  $\tau_0 = 1/5$  as was done above. If we take the values given for the first case ( $\tau_0 = 1/5, v_1 = 1/2, M = \sqrt{3}$ ), then Eq. (46) drives to

$$-\frac{1}{2}v(s)^2 - \frac{3}{2}v(s) - \frac{7}{4} \ln[v(s) - 1/2] + 2 \ln[1 - v(s)] = \frac{4}{5}(s - s_1), \quad (47)$$

where the integration constant is  $s_1 \approx 0.3548$ . Now, the solution must be obtained numerically as it is shown in Table I.

(3) The hard spheres ( $\sigma = 1/2$ ) case was considered by Thomas [6] to criticize Becker’s conclusion that the Boltzmann equation is inadequate to treat strong shocks. He did not obtain a solution for this case but Myong provided the solution in 2014 [10]. In this case the implicit solution is

$$\frac{4}{5}(5\tau_0)^{1/2}(s - s_{1/2}) = \sqrt{4v_1 - v(s)^2} - \frac{v_1 \sqrt{4v_1 - v_1^2}}{v_1 - 1} \ln \left[ \frac{2 \sqrt{4v_1 - v_1^2} \sqrt{4v_1 - v(s)^2} - 2v_1[v(s) - 4]}{v(s) - v_1} \right] + \frac{\sqrt{4v_1 - 1}}{v_1 - 1} \ln \left[ \frac{8v_1 - 2v(s) + 2\sqrt{4v_1 - 1} \sqrt{4v_1 - v(s)^2}}{1 - v(s)} \right] - \arctan \left[ \frac{v(s)}{\sqrt{4v_1 - v(s)^2}} \right] (1 + v_1), \quad (48)$$

TABLE I. Numerical values of the shock wave for  $v$  and  $\rho_n$  at  $\tau_0 = 1/5$  ( $M = \sqrt{3}$ ),  $Pr = 3/4$  for different values of  $\sigma$ .

$s$	$\sigma = 0,$	Eq. (45)	$\sigma = 0,$	Eq. (42)	$\sigma = 1,$	Eq. (47)	$\sigma = 1/2,$	Eq. (49)
	$v$	$\rho_n$	$v$	$\rho_n$	$v$	$\rho_n$	$v$	$\rho_n$
-10.0	0.990	0.011	0.990	0.011	0.978	0.023	0.985	0.015
-9.0	0.984	0.016	0.985	0.016	0.968	0.329	0.978	0.022
-8.0	0.977	0.024	0.977	0.024	0.954	0.048	0.968	0.033
-7.0	0.996	0.035	0.996	0.035	0.936	0.069	0.954	0.049
-6.0	0.950	0.052	0.950	0.052	0.912	0.097	0.934	0.071
-5.0	0.928	0.078	0.928	0.078	0.881	0.135	0.907	0.103
-4.0	0.896	0.116	0.896	0.116	0.845	0.184	0.872	0.147
-3.0	0.854	0.313	0.854	0.171	0.803	0.246	0.828	0.207
-2.0	0.799	0.251	0.799	0.251	0.758	0.320	0.777	0.286
-1.0	0.735	0.361	0.735	0.361	0.711	0.406	0.722	0.385
0.0	0.667	0.500	0.667	0.500	0.667	0.500	0.667	0.500
1.0	0.605	0.653	0.605	0.653	0.626	0.597	0.617	0.621
2.0	0.559	0.789	0.559	0.789	0.592	0.687	0.577	0.735
3.0	0.530	0.887	0.530	0.887	0.565	0.770	0.547	0.827
4.0	0.514	0.944	0.514	0.944	0.544	0.837	0.528	0.895
5.0	0.507	0.974	0.507	0.974	0.530	0.888	0.516	0.938
6.0	0.503	0.988	0.503	0.988	0.519	0.925	0.509	0.965
7.0	0.501	0.994	0.502	0.995	0.513	0.951	0.505	0.980
8.0	0.501	0.998	0.501	0.998	0.508	0.968	0.503	0.989
9.0	0.500	0.999	0.500	0.999	0.505	0.980	0.502	0.994
10.0	0.500	0.999	0.500	1.000	0.503	0.987	0.501	0.997

which is more readily shown using computer algebra to verify Eq. (24) for  $\sigma = 1/2$ . The hard-sphere implicit solution given in Eq. (48) for  $\tau_0 = 1/5$  is written as

$$\sqrt{2 - v(s)^2} + \frac{\sqrt{7}}{2} \ln \left[ \frac{\sqrt{7} \sqrt{2 - v(s)^2} + 4 - v(s)}{v(s) - 1/2} \right] - 2 \ln \left[ \frac{4 - 2v(s) + 2\sqrt{2 - v(s)^2}}{1 - v(s)} \right] - \frac{3}{2} \arctan \left[ \frac{v(s)}{\sqrt{2 - v(s)^2}} \right] = \frac{4}{5} (s - s_{1/2}), \tag{49}$$

where the constant is  $s_{1/2} \approx 0.1192$ . Obviously, the solution is obtained numerically, see Table I.

The particular case of a twofold compression shock wave ( $\tau_0 = 1/5$ ,  $M = \sqrt{3}$ ) has been considered to show that Becker’s implicit solution ( $f(s, v) = 0$ ) can be solved to provide  $v$  as a function of  $s$  but that for the rigid sphere and Maxwell models apparently this is not feasible so that they must be solved numerically. For  $M = \sqrt{3}$ , we have provided numerical values for the explicit and implicit solutions of Becker’s case in Table I. In Figs. 1(a)–1(c) we compared the explicit or implicit solutions with the numerical solution

of the differential equations from which the exact solutions were derived. For  $M = 8$  we found that for the Maxwell model there are cases in which we have been unable to obtain numerical values to the implicit exact solution in some cases, but the numerical solution to the differential equations can be obtained; see Table II.

(4) Implicit solutions for  $\sigma \in \mathbb{N}$  are given by Eq. (36) in terms of a function  $G_n$  defined in Proposition 1, see Eqs. (29), (27), and (28), the result is synthesized by Eq. (37). Apparently this result has not been considered in the literature. As an example we provide the implicit solution for  $\sigma = 2$ :

$$16 \frac{v_1^2 [v_1 \ln(v - v_1) - \ln(1 - v)]}{v_1 - 1} - 8v_1 \left[ \frac{(v_1^2 - 1)v}{v_1 - 1} + \frac{v^2}{2} + \frac{v_1^3 \ln(v - v_1)}{v_1 - 1} - \frac{\ln(1 - v)}{v_1 - 1} \right] + \frac{(v_1^4 - 1)v}{v_1 - 1} + \frac{1}{2} \frac{(v_1^3 - 1)v^2}{v_1 - 1} + \frac{1}{3} \frac{(v_1^2 - 1)v^3}{v_1 - 1} + \frac{1}{4} v^4 + \frac{v_1^5 \ln(v - v_1)}{v_1 - 1} - \frac{\ln(1 - v)}{v_1 - 1} = 20\tau_0^2 (s - s_2). \tag{50}$$

(5) More solutions can be obtained using computer algebra, for example the primitives for several cases such as  $\sigma = 3/2, 5/2, 7/2, 9/2, 11/2$  have been obtained as we did for the hard-spheres model (Maple or Mathematica are able to

find the corresponding primitives), though they are somewhat cumbersome and do not report them here. In cases like  $\sigma = 1/3$  both computer algebra programs failed to provide the primitive.



TABLE II. Numerical values for  $v$  and  $\rho_n$  using the implicit solution, or Eq. (24), at  $\tau_0 = 3/320$  ( $M = 8$ ),  $Pr = 3/4$ , and different values of  $\sigma$ . Eq. (40) is the exact implicit solution for  $\sigma = 0$ , Eq. (48) is the exact implicit solution for  $\sigma = 1/2$ , Eq. (24) is solved for  $\sigma = 0.92$ , Eq. (46) is the exact implicit solution for  $\sigma = 1$ , and Eq. (50) is the exact implicit solution for  $\sigma = 2$ . The results within parentheses correspond to the numerical solution of the first-order one-dimensional differential for  $v$ , Eq. (24), with initial condition  $v(0) = 134/323$  so that  $\rho_n(s_A = 0) = 1/2$ . They are included when the solution to the implicit solution for a given value of  $s_A$  cannot be obtained, in all other cases the solution to the differential equation agrees with results from the implicit solution.  $\rho_n^E$  are the experimental values reported by Steinhilper [50] for Argon.

$s_A$	$\rho_n^E$	Eq. (40)		Eq. (48)		Eq. (24)		Eq. (46)		Eq. (50)	
		$v$	$\rho_n$	$v$	$\rho_n$	$v$	$\rho_n$	$v$	$\rho_n$	$v$	$\rho_n$
-8.0	0.001	1.000	0.000	1.000	0.000	1.000	0.000	(1.000)	0.000	0.458	0.420
-7.0	0.002	1.000	0.000	1.000	0.000	1.000	0.000	(1.000)	0.000	0.452	0.430
-6.0	0.006	1.000	0.000	1.000	0.000	1.000	0.000	(1.000)	0.000	0.446	0.440
-5.0	0.013	1.000	0.000	1.000	0.000	1.000	0.000	(0.979)	0.008	0.441	0.446
-4.0	0.028	1.000	0.000	1.000	0.000	0.966	0.013	0.883	0.047	0.435	0.470
-3.0	0.062	1.000	1.000	1.000	0.000	0.847	0.064	0.763	0.110	0.430	0.460
-2.0	0.133	1.000	0.000	0.995	0.002	0.699	0.152	0.638	0.201	0.425	0.480
-1.0	0.266	0.997	0.001	0.840	0.068	0.548	0.292	0.519	0.329	0.420	0.490
0.0	0.500	0.415	0.500	0.415	0.500	0.415	0.500	0.415	0.500	0.415	0.500
1.0	0.735	0.262	1.000	0.264	0.987	0.324	0.740	0.339	0.692	0.410	0.510
2.0	0.892	0.262	1.000	0.262	1.000	0.281	0.906	0.295	0.849	0.405	0.520
3.0	0.962	0.262	1.000	0.262	1.000	0.267	0.973	0.274	0.939	0.401	0.530
4.0	0.989	0.262	1.000	0.262	1.000	0.263	0.993	0.266	0.976	0.396	0.541
5.0	1.000	0.262	1.000	0.262	1.000	0.262	0.998	0.263	0.992	0.392	0.551
6.0	1.006	0.262	1.000	0.262	1.000	0.262	1.000	0.262	0.997	0.387	0.561
7.0	1.009	0.262	1.000	0.262	1.000	0.262	1.000	0.262	0.999	0.383	0.571

In Tables I and II numerical results for the explicit and implicit exact solutions for different values of  $\sigma$  and  $M$  are provided. They can be used to verify solutions obtained by other means.

Graphs for the implicit and explicit solutions are shown in Fig. 1 for  $\tau_0 = 1/5$ , for the implicit solution we provide only the points that a computer algebra program is able to plot. It should be pointed out that there are two singularities for the implicit solutions corresponding to  $v = 1/2$  or 1, probably this is the origin of the problem. However, solving the differential equation given Eq. (24) provides an alternative method that is free from these problems and provides the solution for the cases in which solving the implicit solution is very difficult. Numerical solutions to Eqs. (15) and (16) are also given, notice that they provide a two-dimensional first-order system of differential equations but that the Morduchow and Libby’s complete integral reduces them to the one-dimensional first-order system given by Eq. (24). It should be pointed out, as the example shows, that there is no guarantee that any of the implicit solutions found (there can be several solutions) gives a shock-wave solution. The existence of the shock-wave solution should be demonstrated by other means when explicit shock-waves solutions cannot be found. Actually, the proof of existence of shock-wave solutions for the NSF constitutive equations was proved, under rather general conditions, by Gilbarg in 1951 [45].

In Fig. 2 the normalized density profiles,  $\rho_n$  versus  $s_A$ , for different values of  $\sigma$  at  $M = 8$  are provided, where  $s_A$  is the distance reduced by Alsmeyer’s mean free path [49]. Its relation to the reduced distance considered here [52] is

$$s = \frac{12}{5\sqrt{2}\pi\tau_0} s_A. \tag{51}$$

For the more realistic case of  $Pr = 2/3$  we have been unable to find exact solutions, either implicit or explicit, in terms of elementary functions or special functions. In this case the numerical solution to the differential Eqs. (15) and (16) seems, up to now, the better alternative.

In addition, the orbits for different Prandtl numbers are shown, as we mentioned above they depend only on the Mach and Prandtl numbers. The direct simulation Monte Carlo (DSMC) method calculations have been shown to have an insight about how they compare with NSF constitutive equations for the soft-sphere model [51,52].

**Entropy change**

The entropy change for this problem can also be calculated from the local equilibrium hypothesis along the shock consistently with the ideal gas equation of state, then

$$\Delta S^*(s_A) = \frac{m}{k_B} [S(s_A) - S_0] = \ln \left\{ \left[ \frac{\tau(s_A)}{\tau_0} \right]^{3/2} \frac{v(s_A)}{v_0} \right\}, \tag{52}$$

where  $S(s_A)$  is the entropy along the shock and  $S_0$  is the entropy at upflow. Recall that  $\tau_0 = \frac{3}{5M^2}$  and  $v_0 = 1$ . It is clear that the entropy change value depends on the Mach number through the  $\tau_0$  dependence. However, either the reduced temperature or the speed can be eliminated by the substitution of the orbit equation written in Eq. (21). As a consequence the entropy change is only a function of one variable and the Mach number, when expressed in terms of the speed it reads

$$\Delta S^*(s_A) = \ln \left\{ \frac{v(s_A)[3 + M^2 - M^2v(s_A)^2]^{3/2}}{3^{3/2}} \right\}. \tag{53}$$

TABLE III. Entropy change profile for  $M = \sqrt{3}$  and different values for the viscosity index. All of them were obtained with the differential equation given by Eq. (24).

$s_A$	$\sigma = 0$	$\sigma = 1/2$	$\sigma = 1$	$\sigma = 3/2$
-10.0	0.000	0.000	0.000	0.001
-9.0	0.001	0.001	0.001	0.002
-8.0	0.001	0.002	0.003	0.004
-7.0	0.003	0.004	0.006	0.010
-6.0	0.007	0.010	0.014	0.023
-5.0	0.016	0.022	0.032	0.049
-4.0	0.035	0.049	0.068	0.095
-3.0	0.076	0.099	0.127	0.159
-2.0	0.148	0.175	0.200	0.222
-1.0	0.234	0.245	0.253	0.258
0.0	0.257	0.257	0.257	0.257
1.0	0.199	0.213	0.224	0.232
2.0	0.159	0.172	0.187	0.202
3.0	0.149	0.154	0.164	0.178
4.0	0.147	0.148	0.153	0.163
5.0	0.146	0.147	0.149	0.154
6.0	0.146	0.146	0.147	0.150
7.0	0.146	0.146	0.147	0.148
8.0	0.146	0.146	0.146	0.147
9.0	0.146	0.146	0.146	0.147
10.0	0.146	0.146	0.146	0.146

It should be noticed that the speed expression and the corresponding values of the entropy change  $\Delta S^*(s_A)$  along the shock wave depend on the viscosity index value. Such values can be obtained explicitly when  $\sigma = 0$  as was shown in the previous section, all other cases will correspond to the speed implicit values. The entropy change  $\Delta S^*(s_A)$  as given in Eq. (53) can be calculated numerically as a function of the distance  $s_A$  as shown in Table III and Fig. 3. Its values have a maximum value at the speed  $v^* = \frac{\sqrt{3+M^2}}{2M}$ , which corresponds to different values of  $s_A$  according to the  $\sigma$  value.

V. SUMMARY AND FINAL REMARKS

The search for exact solutions about the shock-wave structure even in the NSF regime has been a huge challenge in the literature. The efforts to advance along this line began with Taylor’s studies and have gone over numerous steps, giving place to somewhat specific solutions in particular cases. The Becker’s results correspond to a Prandtl number 3/4, where a complete integral is found allowing some exact explicit and implicit solutions. The results in this paper point toward the study of models that go beyond the usual exact solutions, which have considered constant transport coefficients, hard spheres, and Maxwell molecules. We have found a way to consider the soft-spheres model with a viscosity index being any natural number. In particular, for  $Pr = 3/4$  we have shown that there is a countably infinite set of implicit solutions when the viscosity index is zero or a natural number, they include Becker’s ( $\sigma = 0$ ) and the Maxwell model ( $\sigma = 1$ ) implicit solutions as particular cases. For larger values of  $\sigma$  ( $\sigma = 2, 3, \dots$ ) these implicit solutions produce wider normalized

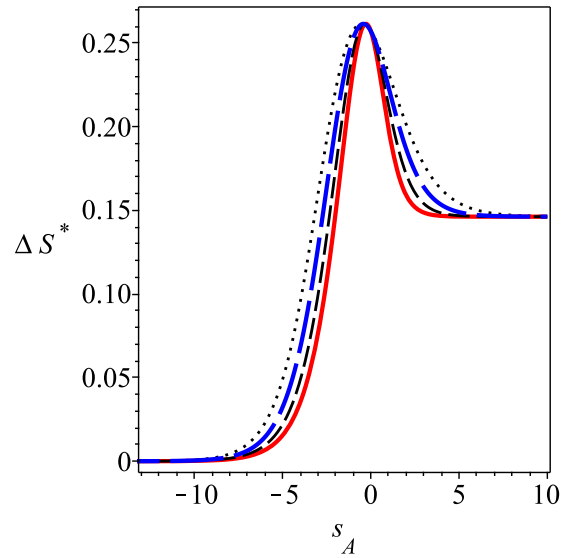


FIG. 3. Entropy change for  $M = \sqrt{3}$  ( $\tau_0 = 1/5$ ) and different values for the viscosity index. Solid line: Explicit solution for  $\sigma = 0$ ; dashed line: solution to Eq. (24) for  $\sigma = 1/2$ ; long dashed line: solution to Eq. (24) for  $\sigma = 1$ ; pointed line: solution to Eq. (24) for  $\sigma = 3/2$ . Its maximum value is the same for all values of  $\sigma$  and it is given as  $\Delta S^*_{max} = 0.261$ , however the  $s_A -$  values where they occur are:  $s_A = -0.277$  ( $\sigma = 0$ ),  $s_A = -0.343$  ( $\sigma = 1/2$ ),  $s_A = -0.424$  ( $\sigma = 1.0$ ),  $s_A = -0.524$  ( $\sigma = 3/2$ ).

density profiles as is exemplified for  $\sigma = 2$  in Table II and Fig. 1(d). Other implicit solutions, which can be obtained with computer algebra, were mentioned but their explicit form has not been provided. A characteristic of the implicit exact solutions found is that they are valid for any Mach number.

Up to the authors knowledge, the previous results were never compared with experiments for the normalized density profiles. Here we illustrate such comparison in the particular case of  $M = 8$  as shown in Fig. 2(a) and Table II for Argon. It is interesting that the Maxwell model provides a relatively good agreement with experiments for such a Mach number though the Prandtl number is equal to 3/4, the hard-sphere model predicts normalized density profiles that are narrow when compared to the experiment. However, a better agreement is obtained when the viscosity index is equal to 0.92 as shown in Fig. 2(a). For comparison we have included a numerical solution to the NSF equations for  $Pr = 2/3$  using a cubic spline to fit the values of the viscosity and thermal conductivity obtained by means of an *ab initio* potential for Argon [23,24]. It is clearly shown in Fig. 2(a) that the NSF equations, with realistic values for the transport coefficients, do not provide an accurate description of the shock-wave profiles as mentioned in the introduction.

Our considerations have been restricted for the steady case but the introduction of time is an important issue, for example in the problem of hydrodynamic stability, and we end by briefly commenting something about this. With respect to the hydrodynamic stability of a plane shock wave the work done by D’yakov and also by Kontorovich in the earlies 1950 must be mentioned [53,54]. As Landau [55] pointed out; they showed that plane shock waves are stable for ripples in

the front shock (sometimes referred as corrugation stability). However, in some cases perturbed nonideal shock waves can become unstable by emitting sound and entropy vortex waves as was shown by Bates and Montgomery for the van der Waals equation, this is now referred to as the D'yakov-Kontorovich instability [56]. At about the same time work done at the National Advisory Committee for Aeronautics (NACA) by several authors, see for example the work done by Moore in 1954 [57], considered also the stability of plane shock waves to perturbation of sound and vorticity that look similar to the corrugation perturbations treated by D'yakov and Kontorovich. This work, initiated at NACA, has been recently explored further in the works by Velikovich and collaborators [58,59] who have reported an analytic linear theory for the interaction of a plane shock wave with either acoustic or turbulent vorticity fields. When the work done at Los Alamos National Laboratory was declassified it became apparent that studies on shock-wave stability were done as early as 1945 [60]. Apart from this, there is a work by Morduchow and Paullay [61] who concluded that plane waves are stable according to the linearized stability theory. For those who are interested in going beyond linear hydrodynamic stability, due to its restrictions, we bring to their attention the mathematical works by Liu on nonlinear stability [62] and end by mentioning the exact nonsteady similarity shock-waves solutions found by Iannelli in 2013 [63]. The previous issues on the hydrodynamic stability of the NSF hydrodynamic model are outside the objectives of this work but constitute a branch that some researchers may want to explore.

#### ACKNOWLEDGMENTS

The authors thank the referees for useful suggestions to improve the paper.

#### APPENDIX

The continuum approach to describe fluid behavior starts with the mass, momentum and energy balance equations,

which are written as [46,55]

$$\frac{\partial \rho}{\partial t} + \nabla \cdot (\rho \mathbf{u}) = 0, \quad (\text{A1a})$$

$$\rho \left( \frac{\partial \mathbf{u}}{\partial t} + \mathbf{u} \cdot \nabla \mathbf{u} \right) = -\nabla \cdot \mathbb{P}, \quad (\text{A1b})$$

$$\rho \left( \frac{\partial e}{\partial t} + \mathbf{u} \cdot \nabla e \right) = -\mathbb{P} : \nabla \mathbf{u} - \nabla \cdot \mathbf{q}, \quad (\text{A1c})$$

where the local variables are  $\rho \equiv \rho(\mathbf{r}, t)$  the mass density,  $\mathbf{u} \equiv \mathbf{u}(\mathbf{r}, t)$  the hydrodynamic velocity,  $e(\mathbf{r}, t)$  the internal energy per unit mass,  $\mathbb{P} \equiv \mathbb{P}(\mathbf{r}, t)$  the pressure tensor and  $\mathbf{q}(\mathbf{r}, t)$  the heat flux, all of them may depend on position and time,  $\mathbf{r}$  and  $t$ . The term  $\mathbb{P} : \nabla \mathbf{u} \equiv \mathbb{P}_{ij} \partial_j u_i$  represents the full contraction of the involved tensors, where Einstein convention is used.

Now, we consider the particular case of the hydrodynamic Eq. (A1c) for a longitudinal wave that propagates with constant velocity  $c$ , in the specific direction  $\hat{\mathbf{i}}$ . We use similarity ideas and take the ansatz  $\mathbf{u}(\mathbf{r}, t) = u(x - ct)\hat{\mathbf{i}}$ ,  $\rho(\mathbf{r}, t) = \rho(x - ct)$ ,  $\mathbb{P} = P_{xx}(x - ct)\hat{\mathbf{i}}\hat{\mathbf{i}}$ ,  $e(\mathbf{r}, t) = e(x - ct)$ , and  $\mathbf{q}(\mathbf{r}, t) = q(x - ct)\hat{\mathbf{i}}$ , where  $\mathbf{r} = x\hat{\mathbf{i}} + y\hat{\mathbf{j}} + z\hat{\mathbf{k}}$  [64]. Substitution of it in Eqs. (A1a), (A1b), and (A1c) leads to

$$-c\rho' + (\rho u)' = 0, \quad (\text{A2a})$$

$$\rho(-c u' + u u') = -P'_{xx}, \quad (\text{A2b})$$

$$\rho(-c e + u e') = -P_{xx} u' - q', \quad (\text{A2c})$$

where the prime denotes the derivative with respect to  $\xi \equiv x - ct$ . Here we will be interested in an steady shock wave in which the equations are independent of time. In this case Eqs. (A2) simplify by means of the choice of a reference system in which the speed  $c$  is equal zero. The resulting one-dimensional differential equations can be integrated to yield the well-known constant fluxes of mass, momentum, and energy for a shock wave, as written in Eqs. (1).

- 
- [1] M. D. Salas, *Shock Waves* **16**, 477 (2006).
  - [2] L. Rayleigh, *Proc. R. Soc. London, Series A* **84**, 247 (1910).
  - [3] G. I. Taylor, *Proc. R. Soc. London, Series A* **84**, 371 (1910).
  - [4] R. Becker, *Z. Phys.* **8**, 321 (1922).
  - [5] R. Becker, Technical Report 506, National Advisory Committee for Aeronautics, Washington (1929), from *Zeitschrift für Physik*, Vol. VIII.
  - [6] L. H. Thomas, *J. Chem. Phys.* **12**, 449 (1944).
  - [7] M. Morduchow and P. A. Libby, *J. Aero. Sci.* **16**, 674 (1949).
  - [8] B. M. Johnson, *J. Fluid Mech.* **726**, R4 (2013).
  - [9] B. M. Johnson, *J. Fluid Mech.* **745**, R1 (2014).
  - [10] R. S. Myong, *AIAA J.* **52**, 1075 (2014).
  - [11] A. Patel and M. Singh, *Shock Waves* **29**, 427 (2018).
  - [12] S. Chapman and T. G. Cowling, *The Mathematical Theory of Non-Uniform Gases* (Cambridge University Press, Cambridge, 1970).
  - [13] D. Gilbarg and D. Paolucci, *J. Rational Mech. Anal.* **2**, 617 (1953).
  - [14] H. M. Mott-Smith, *Phys. Rev.* **82**, 885 (1951).
  - [15] H. Grad, *Commun. Pure Appl. Math.* **5**, 257 (1952).
  - [16] D. Burnett, *Proc. London Math. Soc.* **39**, 385 (1935).
  - [17] C. S. Wang-Chang, in *Studies in Statistical Mechanics*, edited by J. de Boer and G. E. Uhlenbeck (North-Holland, Amsterdam, 1970), Vol. 5, p. 27.
  - [18] G. A. Bird, *Molecular Gas Dynamics and the Direct Simulation of Gas Flows* (Oxford-Clarendon, New York, 1994).
  - [19] G. A. Bird, *The DSMC Method (Ver. 1.2)* (G.A. Bird, Lexington, KY, 2013).
  - [20] W. G. Hoover, *Phys. Rev. Lett.* **42**, 1531 (1979).
  - [21] E. Salomons and M. Mareschal, *Phys. Rev. Lett.* **69**, 269 (1992).
  - [22] F. Sharipov and C. Dias, *Comput. Fluids* **150**, 115 (2017).
  - [23] K. Patkowski and S. Krzysztof, *J. Chem. Phys.* **133**, 094304 (2010).

- [24] B. Song, X. Wang, and Z. Liu, *Mol. Simul.* **42**, 9 (2016).
- [25] M. S. Shavaliyev, *J. Appl. Maths. Mechs.* **63**, 427 (1999).
- [26] L. S. García-Colín, R. M. Velasco, and F. J. Uribe, *Phys. Rep.* **465**, 149 (2008).
- [27] M. S. Shavaliyev, *J. Appl. Maths Mechs* **57**, 573 (1993).
- [28] F. J. Uribe, R. M. Velasco, and L. S. García-Colín, *Phys. Rev. Lett.* **81**, 2044 (1998).
- [29] F. J. Uribe, R. M. Velasco, L. S. García-Colín, and E. Diaz-Herrera, *Phys. Rev. E* **62**, 6648 (2000).
- [30] K. A. Fisco and R. D. Chapman, in *Rarefied Gas Dynamics*, edited by E. P. Muntz, D. P. Weaver, and D. H. Campbell (AIAA, Reston, VA, 1989), pp. 374–395.
- [31] R. K. Agarwal, K. Y. Yun, and R. Balakrishnan, *Phys. Fluids* **13**, 3061 (2001).
- [32] Z. Cai, R. Li, and Y. Wang, *Commun. Comput. Phys.* **11**, 1415 (2012).
- [33] N. Singh, R. S. Jadhav, and A. Agrawal, *Phys. Rev. E* **96**, 013106 (2017).
- [34] A. V. Bobylev, *Phil. Trans. R. Soc. A* **376**, 20170227 (2018).
- [35] I. Müller and T. Ruggeri, *Extended Thermodynamics* (Springer-Verlag, New York, 1993).
- [36] H. Struchtrup, *Macroscopic Transport Equations for Rarefied Gas Flows: Approximation Methods in Kinetic Theory*, Interaction of Mechanics and Mathematics (Springer, Berlin, 2005).
- [37] M. Torrilhon, *Annu. Rev. Fluid Mech.* **48**, 429 (2016).
- [38] M. Y. Timokhin, H. Struchtrup, A. A. Kokhanchik, and Y. A. Bondar, *Phys. Fluids* **29**, 037105 (2017).
- [39] M. Al-Ghoul and B. C. Eu, *Phys. Rev. E* **56**, 2981 (1997).
- [40] H. Brenner, *Physica A* **349**, 60 (2005).
- [41] H. Brenner, *Physica A* **388**, 3391 (2009).
- [42] C. J. Greenshields and J. M. Reese, *J. Fluid Mech.* **580**, 407 (2007).
- [43] L. G. Margolin, *Entropy* **19**, 368 (2017).
- [44] G. Emanuel, *Shock Waves* **25**, 11 (2015).
- [45] D. Gilbarg, *Am. J. Math.* **73**, 256 (1951).
- [46] Y. B. Zel'dovich and Y. P. Raizer, *Physics of Shock Waves and High-Temperature Hydrodynamic Phenomena* (Dover, New York, 2002).
- [47] H. Hamad, *Proc. R. Soc. London A* **452**, 2163 (1996).
- [48] M. W. Liebeck, in *The Princeton Companion to Mathematics*, edited by T. Gowers, J. Barrow-Green, and I. Leader (Princeton University Press, Princeton, NJ, 2008), Chap. 5, pp. 708–710.
- [49] H. Alsmeyer, *J. Fluid Mech.* **74**, 497 (1976).
- [50] E. A. Steinhilper, Electron beam measurements of the shock wave structure, Ph.D. thesis, California Institute of Technology (1971).
- [51] F. J. Uribe and R. M. Velasco, *Phys. Rev. E* **97**, 043117 (2018).
- [52] R. M. Velasco and F. J. Uribe, *Phys. Rev. E* **99**, 023114 (2019).
- [53] S. P. D'Yakov, *Zh. Eksp. Teor. Fiz.* **27**, 288 (1954).
- [54] V. M. Kontorovich, *Zh. Eksp. Teor. Fiz.* **33**, 1525 (1957) [*Soviet Physics JEPT* **6**, 1179 (1958)].
- [55] L. D. Landau and E. M. Lifshitz, *Fluid Mechanics* (Pergamon Press, London, 1959).
- [56] J. W. Bates and D. C. Montgomery, *Phys. Rev. Lett.* **84**, 1180 (2000).
- [57] F. K. Moore, National Advisory Committee for Aeronautics Report No. 1165, 1954.
- [58] C. Huete, J. G. Wouchuk, and A. L. Velikovich, *Phys. Rev. E* **85**, 026312 (2012).
- [59] J. G. Wouchuk, C. Huete Ruiz de Lira, and A. L. Velikovich, *Phys. Rev. E* **79**, 066315 (2009).
- [60] A. E. Roberts, Los Alamos Scientific Report No. LA-299, 1945.
- [61] M. Morduchow and A. J. Paullay, *Phys. Fluids* **14**, 323 (1971).
- [62] T.-P. Liu, *Commun. Pure App. Math.* **39**, 565 (1986).
- [63] J. Iannelli, *Int. J. Numer. Meth. Fluids* **72**, 157 (2013).
- [64] G. I. Barenblatt, *Scaling, Self-similarity, and Intermediate Asymptotics*, (Cambridge University Press, Cambridge, 1996).